Journal of Loss Prevention in the Process Industries 22 (2009) 868–872

Contents lists available at ScienceDirect

Journal of Loss Prevention in the Process Industries

journal homepage: www.elsevier.com/locate/jlp

Safety assessment based on mapping of degraded mechanical properties of materials for power plant pipeline using instrumented indentation technique

Kyung-Woo Lee [a,*], Kug-Hwan Kim [a], Ju-Young Kim [a], Kwang-Ho Kim [b], Byung-Hak Choi [c], Dongil Kwon [a]

[a] Department of Materials Science & Engineering, Seoul National University, Seoul 151-744, Republic of Korea
[b] Frontics Inc., Research Institute of Advanced Materials, Seoul National University, Seoul 151-744, Republic of Korea
[c] Department of Metal and Materials Engineering, College of Engineering, Kangnung University, Kangnung, Republic of Korea

ARTICLE INFO

Article history:
Received 15 August 2007
Received in revised form
19 August 2008
Accepted 17 September 2008

Keywords:
Safety assessment
Instrumented indentation technique
Degraded mechanical properties
Power plant pipelines

ABSTRACT

The remaining life prediction of those is accomplished by accelerated degradation tests such as creep testing. However, creep testing is both time-consuming and expensive and hence impossible to apply under industrial conditions, where prompt management and analysis are necessary. While residual lifetime predictions and safety assessments of power plant facilities are made using standard mechanical testing methods such as uni-axial tensile and fracture mechanics tests. However, these tests cannot be applied to in-service structure components because of their destructive nature. A nondestructive instrumented indentation technique is thus attractive for investigating the mechanical properties of in-service systems. This technique can measure flow properties by analyzing indentation load-depth curves reflecting the deformation behavior of the material beneath the rigid spherical indenter. In this study, heat treatment was used to produce degraded samples of X20CrMo12.1V and SA-213 T23, materials widely used in power plant pipelines, and their mechanical properties versus degree of degradation were evaluated by instrumented indentation. We assess the degradation of mechanical properties by microstructural analysis and discuss the possibility of appraising the safety of power plant facilities by in-situ monitoring of mechanical properties using instrumented indentation testing.

1. Introduction

A large fraction of power, petroleum, and chemical plants the world over have been in operation so long that their critical components have been used beyond a design life of 30–40 years. Lifetime prediction and safety assessment of these plants have attracted recent interest because of the frequent failure of structural components by time-dependent degradation in a severe operating environment. Lifetime prediction is generally done by accelerated degradation tests such as creep and stress-rupture test, etc. However, these methods have many drawbacks: they are time-consuming and expensive, unsuitable for use in industrial conditions because they are destructive, removal and testing of samples are difficult, and data on mechanical properties are unavailable for the component's service-degraded conditions (e.g. weldments) (Viswanathan, 1989). Many kinds of nondestructive techniques, such as replica analysis, electronic resistance test and ultrasonic test, have been developed for this same purpose, but they also have many drawbacks. For example, nondestructive methods are needed to determine properties in a specific component. In welded components, the problem is further compounded by the fact that a weldment contains a complex microstructure of many zones with varying material properties. With these difficulties in indirect measurement of mechanical property degradation, several nondestructive methods have been used to evaluate microstructural degradation in order to predict mechanical property change and thus remaining lifetime. Converting microstructural change to mechanical property change in this way requires a well-established database because this conversion depends very strongly on empirical relationships between microstructure and mechanical properties (Jang, Choi, Lee, & Kwon, 2005).

The present work adopts an instrumented indentation test to measure mechanical property degradation, a technique developed as a potential method for nondestructive testing of in-field structures. This technique can measure various mechanical properties such as hardness, elastic modulus, tensile properties, residual stress, and fracture toughness by analyzing the indentation load-depth curve as shown in Fig. 1 (Ahn & Kwon, 2001; Kim, Lee, Lee, & Kwon, 2006; Lee et al., 2006; Lee & Kwon, 2004; Oliver & Pharr, 1992; Suresh & Giannakopoulos, 1998). Indentation testing can be made portable, so that nondestructive, in-situ, on-site testing would be available, with relatively little sample preparation.

* Corresponding author. Tel.: +82 2 880 8404; fax: +82 2 886 4847.
E-mail address: case77@snu.ac.kr (K.-W. Lee).

0950-4230/$ – see front matter © 2008 Elsevier Ltd. All rights reserved.
doi:10.1016/j.jlp.2008.09.007

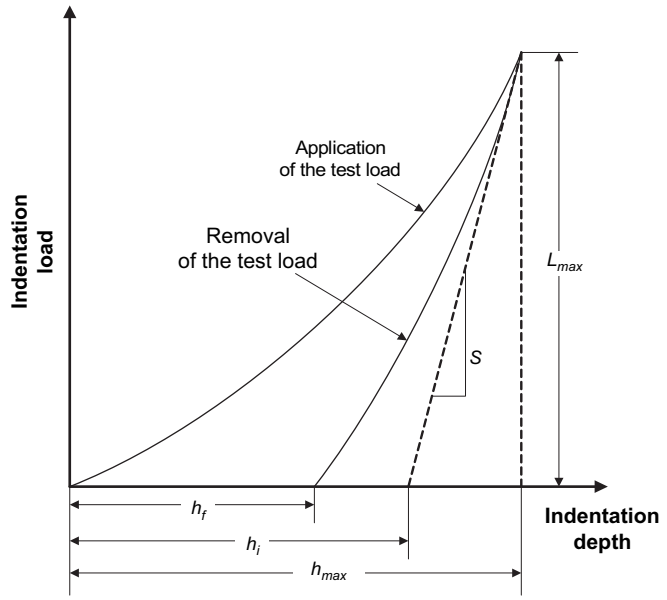

Fig. 1. Schematic graph of indentation load-depth curve.

Similarly, lifetime monitoring of real structures would also become available with relatively little or no sample preparation.

In this work, instrumented indentation testing was used to investigate the relation between a material's mechanical properties and degree of degradation. After heat treatment to produce degraded materials, the degraded mechanical properties are analyzed in microstructural terms. We suggest the possibility of safety assessment of on-site materials by mechanical property measurement using instrumented indentation testing.

2. Evaluation of tensile properties by instrumented indentation

Tensile properties can be evaluated by defining representative stress and strain with parameters obtained from instrumented indentation tests using a spherical indenter (Ahn & Kwon, 2001; Kim et al., 2006). The accuracy of this approach depends strongly on how the contact depth is analyzed and how the representative stress and strain are defined. Our detailed investigation into evaluating the tensile properties is described below.

A contact depth h_c^* at maximum indentation load can be evaluated by analyzing the unloading curve in Fig. 1 using the concepts of indenter geometry and elastic deflection (Oliver & Pharr, 1992):

$$h_c^* = h_{\max} - \omega(h_{\max} - h_i) \quad (1)$$

where h_i is the intercept indentation depth and the indenter shape parameter ω is 0.75 for a spherical indenter. The material pile-up around the indentation enlarges the contact radius (from the analysis of elastic deflection). The extent of this pile-up is determined by the work-hardening exponent n and the indentation depth ratio h_{max}/R:

$$h_{\text{pile}} = h_c^* \times f(n,\ h_{\max}/R) \quad (2)$$

With these parameters, the representative strain and stress are determined as follows. On the basis of the deformation shape and

Table 1
Chemical compositions of materials used.

Material	C	Si	Mn	Cr	Mo	Ni	V	Nb	W
X20CrMo12.1V	0.2	0.3	0.5	11.2	1.0	0.5	0.3	–	–
SA-213 T23	0.06	0.20	0.45	2.25	0.1	–	0.25	0.05	1.6

Table 2
Design of accelerated degradation testing and operating conditions.

Material	Design for accelerated heat treatments		Operating temperature (K)	Allowable temperature (K)
	Time (h)	Temperature (K)		
X20CrMo 12.1V	10, 100, 1000	923, 973, 1023, 1073	813–843	973
SA-213 T23	10, 100, 1000	873, 923, 973, 1023, 1073	823	933

Table 3
Tensile properties obtained from uni-axial tensile tests and instrumented indentation tests (note: Symbols YS and UTS mean the true values of tensile properties).

Materials	YS (MPa)			UTS (MPa)		
	Tensile	IIT	Error (%)	Tensile	IIT	Error (%)
X20	534.6	566.3	−5.93	859.8	837.2	2.63
T23	497.1	500.8	−0.74	675.4	638.4	5.48

strain distribution under a spherical indenter, Ahn and Kwon (2001) proposed a new definition using the tangent function. The displacement u_z, along the depth axis under the indenter can be expressed geometrically as:

$$u_z = h - \left(R - \sqrt{R^2 - r^2}\right), \quad (3)$$

where R is the indenter radius and r is a radius at any point on the depth axis. The shear strain is derived by differentiating the

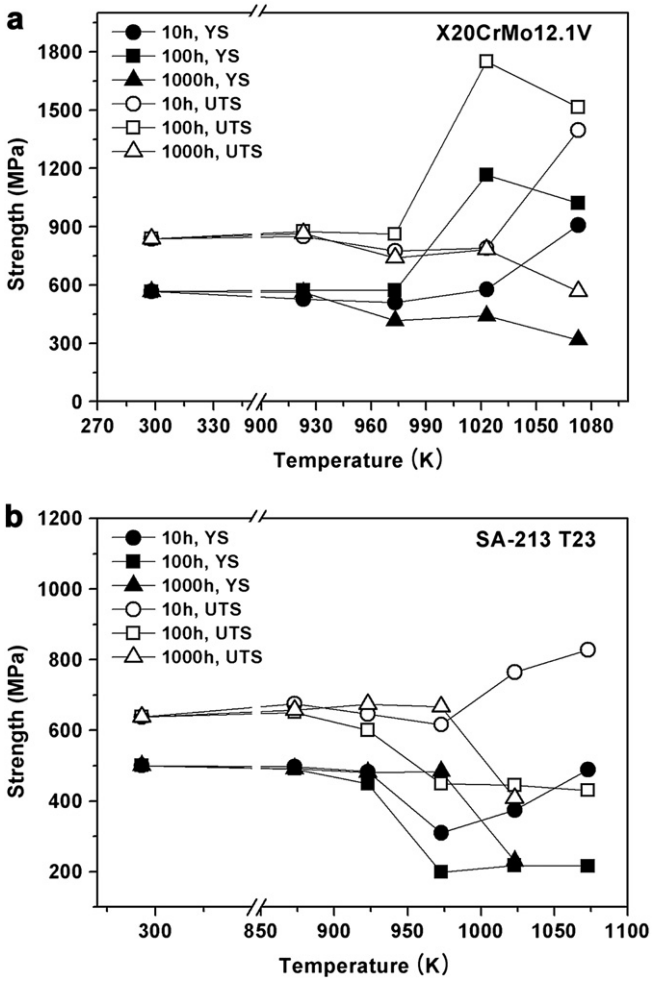

Fig. 2. Deviations of degradation time and temperature on yield strength and ultimate tensile strength.

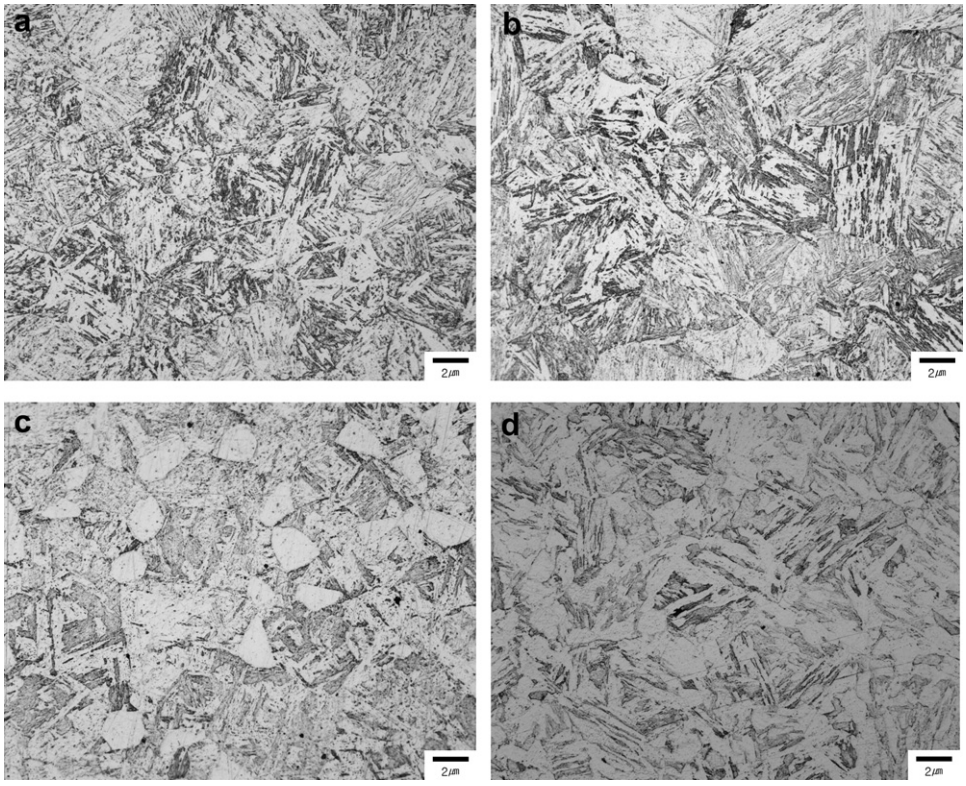

Fig. 3. Microstructure of X20 degraded for 100 h at (a) 923 K, (b) 973 K, (c) 1023 K, (d) 1073 K.

displacement in the depth direction. The maximum shear strain is obtained at $r = a_c$, and Ahn and Kwon (2001) obtained the true strain by using a strain-proportional constant α:

$$\varepsilon_R = \left(\frac{\alpha}{\sqrt{1-(a_c/R)^2}}\right)\left(\frac{a_c}{R}\right) = \alpha\tan\gamma, \quad (4)$$

where a_c is contact radius; α was determined as 0.14 for various materials by FEA (Jeon, Baik, Kim, Lee, & Kwon, 2005).

Since the elastic and elastic/plastic deformation stages in steels generally occur at very low indentation loads, only the plastic deformation stage is considered here. The mean pressure P_m obtained by dividing the maximum load L_{max} by the contact area is well known to be about three times the representative stress σ_R for fully plastic deformation of steels (Ahn & Kwon, 2001; Tabor, 1951). In other words, the representative stress can be expressed as:

$$\sigma_R = \left(\frac{1}{\Psi}\right)P_m = \left(\frac{1}{\Psi}\right)\left(\frac{L_{max}}{\pi a_c}\right), \quad (5)$$

where Ψ is a plastic constraint factor, here taken as 3.

The true stress and strain points obtained by the indentation test are fitted to a constitutive equation (a simple power-law-type Hollomon equation, $\sigma = K\epsilon^n$), and K, a material constant, and n, the work-hardening exponent, are determined. Since the elastic modulus is obtained by indentation testing (Oliver & Pharr, 1992), the yield strength can be measured from the intersection point of the flow curve and a line with a slope of the elastic modulus 0.2% offset from the origin. The ultimate tensile strain should be same as the work-hardening exponent, by the theory of instability in

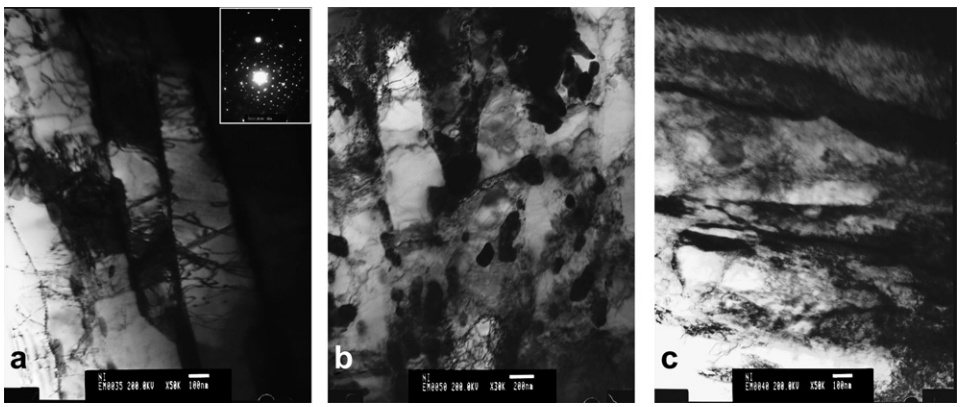

Fig. 4. TEM micrographs of X20 degraded for 100 h at (a) 923 K, (b) 973 K, (c) 1023 K.

tension (Dieter, 1986), and from this the tensile strength can be determined. However, the algorithms can be applied only to power-law hardening materials obeyed by the Hollomon equation (Lee, Kim, Kim, & Kwon, 2008).

3. Experimental procedure

The specimens used here were X20CrMo12.1V and SA-213 T23 (below called X20 and T23), widely used in power plant pipelines; chemical compositions are given in Table 1. Heat treatment was performed at various temperatures and times to produce the accelerated-aged specimens described in Table 2. Specimens used in degradation testing were divided into four equal with circumference after cutting them in 100-mm lengths. The heat treatment condition was designed in accordance with allowable temperatures and operating temperatures. The aged condition of X20 was designed with minimum temperature, 923 K (allowable temperatures between 873 and 973 K) to maximum temperature, 1073 K for 10, 100 and 1000 h; that of T23 was designed with the same conditions with the exception of minimum temperature, 873 K (allowable temperatures between 843 and 933 K).

Instrumented indentation tests were carried out with a portable indentation system, AIS 2100 (Frontics Inc., South Korea). The indenter was a tungsten-carbide ball of 0.25-mm radius, and indentation speed was 0.3 mm/min. The final maximum depth was 0.15 mm and 15 multiple unloadings down to 50% of maximum load at each point were applied. Indentation testing was performed at room temperature. To observe the microstructure in an optical microscope, the specimen surface was polished with 1-μm Al_2O_3 powder and chemically etched. Since destructive sample preparation was available, uni-axial tensile tests were performed by Instron 5584 (Instron Inc., MA, USA) to confirm the flow properties measured by IIT. Uni-axial tensile testing was performed with a rectangular shape specimen with a gauge length of 25 mm, with a loading rate of 1 mm/min.

4. Results and discussion

4.1. Mechanical properties

Table 3 shows the values of yield strength (σ_Y) and ultimate tensile strength (σ_{UTS}) measured by instrumented indentation testing and uni-axial tensile testing before accelerated heat treatments. They are in very good agreement within ±5%, which shows the reasonable means to measure flow properties of materials in-use only with IIT. Fig. 2 shows the effect of degradation time and temperature on the yield strength and ultimate tensile strength obtained in the indentation tests. Results for both materials showed the same variation in both the yield and ultimate tensile strength at each degradation time condition. While the values of yield and ultimate tensile strength of X20 for 1000 h decrease with increasing aging temperature, those for 10 h and 100 h increase over a specified temperature range, 1073 and 973 K, respectively. For T23, the strength for 1000 h decreases after saturation at 973 K. Against this, those in other conditions decreases until 973 K, and then showed with increasing or saturating at temperature more than 973 K.

The mechanical properties of carbon steel or low-alloy steel are known to be generally reduced by long-term exposure to high temperatures by the growth of spheroidized pearlite or coarsened fine carbides (ASME B&PV Part A, 2004). However, the present results show different behavior except at 1000 h. This may be caused by another degradation mechanism in this temperature region, as discussed in Section 4.2 below.

4.2. Microstructure

Fig. 3 shows the microstructure of X20 degraded for 100 h at each temperature condition. The microstructure over all

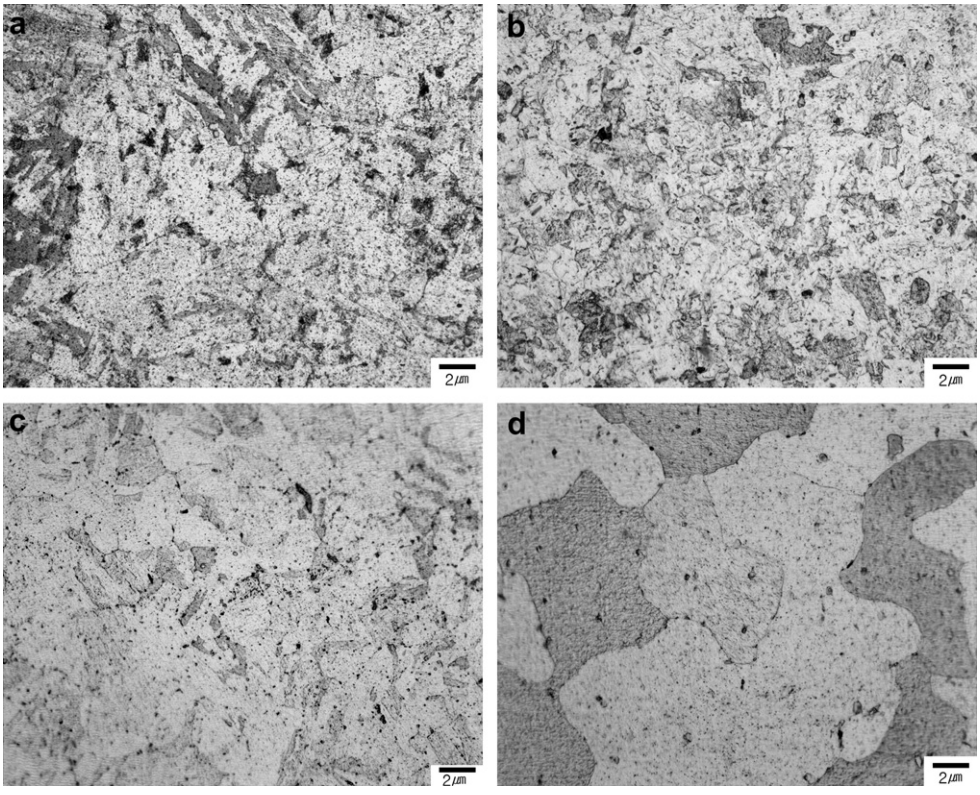

Fig. 5. Microstructure of T23 degraded for 10 h at (a) 1023 K and (b) 1073 K, for 100 h at (c) 973 K and (d) 1023 K.

temperature regions is observed to be tempered martensite, which are fine-constituent dispersions of Fe_3C in α-ferrite sites. It also appears to be lath-shaped in alternate light and dark layers. The lath size increases with degradation time and its size coarsens. However, the microstructure of X20 showed no significant differences despite changes in temperature, that is, the overall optical microscope observations do not correlate with the relations between the microstructure and the mechanical property variation. Hence, TEM (transmission electron microscope) was used for more precise examination. TEM micrographs of X20 in different degradation states are shown in Fig. 4. Carbide appears to the shape of dispersed particle in several or the shape of film; they are evaluated as $M_{23}C_6$ by analyzing SAED patterns. Also, they coarsened with increasing time because of the effect of Cr and Mo components (Seok & Koo, 2005): the coarsened carbides increase the dislocation mobility because of increased intercarbide spacing, thus decreasing the strength. For 100 h condition at 1023 K, however, the coarsened carbides disappeared and needle carbides of M_3C type in lath were observed. Eventually, the increase of strength of X20 in 10 and 100 h above 973 K is caused by the precipitated carbides in lath.

Fig. 5 show the microstructure of T23 degraded for 10 h at 1023 and 1073 K and for 100 h at 973 and 1023 K. The microstructure is a mixture of ferrite (α, light) and pearlite ($\alpha + Fe_3C$, dark). At conditions above 973 K, however, this microstructure was transformed into ferrite (α) and austenite (γ) phases, since the transformation temperature (996 K) (Reed-Hill, 1991) was exceeded, and then the γ-phase transformed again to pearlite after cooling to room temperature. In this long-duration high-temperature condition, the grain of α- and γ-phases is coarsened and the coarsening is maintained (see Fig. 5(d)), even through the γ-phase transforms to pearlite after cooling. This grain coarsening is one of the causes of the decline in mechanical properties, as in the 100 and 1000 h conditions above 973 K. On the other hand, the increase of strength in 10 h condition above 973 K is attributed to the dispersed carbides. In other words, in this condition the cementite (Fe_3C) in pearlite decomposes into fine carbide that is dispersed into the α-ferrite matrix. This dispersion-hardening mechanism causes the increasing strength in 10 h condition above 973 K. This effect is brought out well in 10 h condition because the effect of grain coarsening for 10 h is much smaller than for other times.

According to the above results, the increase or decrease in strength occurred due to the change in microstructure by degradation above 973 K. Otherwise, the effect of degradation below 973 K on the strength and the microstructure was insignificant. This means that degree of material degradation is able to expect through measurement of the yield and ultimate tensile strength.

As an application example, we measured the strength of X20 real used for 70,000 h at steam power plant by instrumented indentation test. The yield and ultimate tensile strength are 547 and 871 MPa, respectively. According to the criteria in the present work, the material used is secure from degradation. In conclusion, the measurement of strength using instrumented indentation, which estimates the degree of degradation by monitoring the strength variation and indicates a criterion for refurbishment and replacement, show good potential for safety assessment of on-site facilities.

5. Conclusion

Heat treatment was performed to degrade X20CrMo12.1V and SA-213 T23 samples. The degraded material properties such as yield strength and ultimate tensile strength were measured by instrumented indentation test and the microstructures were observed by OM and TEM. The values of strength of both materials increase with increasing degradation temperature at particular time condition. These strength variations are verified by the analysis of microstructure, for example, the generation of precipitated carbides and the effect of dispersed carbides etc. Also, we diagnosed the safety of X20 real used for 70,000 h at steam power plant on the basis of this work. The results are estimated that X20 real used is secure from degradation, that is, confirm the excellent potential of instrumented indentation for safety assessment, i.e. in-situ monitoring of material properties of on-site facilities.

Acknowledgement

This research was supported by a grant (02K1401-01321) from Center for Nanoscale Mechatronics & Manufacturing, one of the 21st Century Frontier Research Programs, which are supported by Ministry of Education, Science and Technology, KOREA.

References

Ahn, J. H., & Kwon, D. (2001). Derivation of plastic stress-strain relationship from ball indentation: examination of strain definition and pileup effect. *Journal of Materials Research, 16*, 3170–3178.

ASME B&PV Part A. (2004). *Specification for seamless ferritic and austenitic alloy-steel boiler, superheater and heat-exchanger*. ASME.

Dieter, G. E. (1986). *Mechanical metallurgy* (SI Metric ed.). New York: McGraw Hill.

Jang, J.-I., Choi, Y., Lee, Y. H., & Kwon, D. (2005). Instrumented microindentation studies on long-term aged materials; work-hardening exponent and yield ratio as new degradation indicators. *Material Science Engineering A, 395*, 295–300.

Jeon, E.-C., Baik, M.-K., Kim, S.-H., Lee, B.-W., & Kwon, D. (2005). Determining representative stress and representative strain in deriving indentation flow curves based on finite element analysis. *Key Engineering Materials, 297-300*, 2152–2157.

Kim, J.-Y., Lee, K.-W., Lee, J.-S., & Kwon, D. (2006). Determination of tensile properties by instrumented indentation technique: representative stress and strain approach. *Surface and Coating Technology, 201*, 4278–4283.

Lee, J.-S., Jang, J.-i., Lee, B.-W., Choi, Y., Lee, S.-G., & Kwon, D. (2006). An instrumented indentation technique for estimating fracture toughness of ductile materials: a critical indentation energy model based on continuum damage mechanics. *Acta Materialia, 54*, 1101–1109.

Lee, K.-W., Kim, K.-H., Kim, J.-Y., & Kwon, D. (2008). Derivation of tensile flow characteristics for austenitic materials from instrumented indentation technique. *Journal of physics D: Applied physics, 41*. 074014.

Lee, Y.-H., & Kwon, D. (2004). Estimation of biaxial surface stress by instrumented indentation with sharp indenters. *Acta Materialia, 52*, 1555–1563.

Oliver, W. C., & Pharr, G. M. (1992). An improved technique for determining hardness and elastic modulus using load and displacement sensing indentation experiment. *Journal of Materials Research, 7*, 1564–1583.

Reed-Hill, R. E. (1991). *Physical metallurgy principles*. USA: PWS.

Seok, C. S., & Koo, J. M. (2005). Evaluation of material degradation of 1Cr-1Mo-0.25V steel by non-destructive method. *Material Science Engineering A, 395*, 141–147.

Suresh, S., & Giannakopoulos, A. E. (1998). A new method for estimating residual stresses by instrumented sharp indentation. *Acta Materialia, 46*, 5755–5767.

Tabor, D. (1951). *Hardness of metals*. UK: Clarendon Press.

Viswanathan, R. (1989). *Damage mechanisms and life assessments of high-temperature components*. ASM International.